Spacing of Cracks in Reinforced Concrete

By Zdeněk P. Bažant,[1] F. ASCE and Byung H. Oh[2]

Abstract: The spacing and width of cracks in a parallel crack system is approximately analyzed using the energy criterion of fracture mechanics as well as the strength criterion. The energy criterion indicates that the crack spacing is a function of the axial strain of the bars and also depends on bar spacing, bar diameter, fracture energy of concrete, and its elastic modulus. Both the energy and strength criteria yield a minimum strain necessary to produce any cracks. The energy criterion and the bond slip conditions further yield a lower bound on possible spacing of continuous cracks. The rules for the formation of shorter, partial length, cracks are also set up. Approximate expressions for the crack width at, and away, from the bars are derived. Numerical comparisons indicate satisfactory agreement with existing test data, and lend theoretical support to one aspect of the empirical Gergely-Lutz formula obtained by statistical regression analysis of test data. Finally, formation of skew cracks in a biaxially stressed and biaxially reinforced plate is analyzed and a crack spacing formula is derived for one typical case.

Introduction

The width and spacing of cracks in parallel crack systems in reinforced concrete structures have a major influence on structural performance, including shear, tensile and bending stiffnesses, energy absorption capacity, ductility, and corrosion resistance of reinforcement. Much has been learned already about crack width and spacing (1,2,5–14,16,18–20,22–25,29,30), but a completely rational and general method of prediction is still unavailable. We will attempt here an advance in this direction, paying particular attention to crack spacing since it is already known reasonably well how to calculate the width once the crack spacing is determined, e.g., as is shown in an earlier study of tension-stiffening (5).

The existing formulas for the spacing of cracks (2,11–13,18) are based on the strength criterion. The need for empirical relations suggests, however, that the strength concept may be insufficient. Theoretically, cracking is fracture and so the energy required to form the cracks should be also taken into account. As we will see, this gives reasonable results where the strength concept does not. The energy approach has already been used to derive a formula for the spacing of thermal cracks in rock (8,10) and of drying cracks in concrete (7). We will employ here a similar approach, restricting our attention to cracks caused by applied loads.

Cracking Criterion

Applicability of fracture mechanics to concrete has been denied by most specialists because of negative experimental evidence. However, some recent researchers, e.g., Hillerborg, et al. (17), Petersson (26), A. Ingraffea (private communications, 1981, 1982), and the writers (3), indicate that a satisfactory agreement with essentially all fracture test data can be achieved provided one takes into account the fact that, due to material heterogeneity, the fracture process zone is long, spanning a length of at least several aggregate sizes. As a consequence of this fact, the linear fracture mechanics cannot be used (except for very large structures such as dams) and the energy criterion of fracture mechanics, as well as the strength criterion, must be applied globally over regions that measure at least several aggregate sizes. This is clear even without experimental evidence, since structural analysis implies the hypothesis of smoothing of a heterogeneous material by an equivalent homogeneous continuum in which, if one uses the language of the statistical theory of randomly heterogeneous materials, the stresses and strains must be understood as the averages of the actual stresses and strains in the microstructure over the so-called representative volume whose size must be taken to be at least several times the size of the inhomogeneities. On a smaller scale, the continuum concepts are meaningless.

When the fracture process zone is not negligibly small, one must take into account the stress-strain relation of the material, including the decline of stress to zero at very large strains (strain-softening). Its two principal characteristics, which seem sufficient for most practical purposes, are the tensile strength, f'_t (determined as the peak stress in direct tension tests), and the fracture energy, $\mathcal{G}_f$, which equals approximately the area under the stress-strain diagram times the effective width of the fracture process zone, thus depending on the mean slope of the strain-softening segment of stress-strain relation. The microcracking which must precede fracture formation begins to form approximately at the peak stress point, and fracture obviously cannot form if the strength (peak stress) is not reached. So the strength criterion (applied, of course, to the average stress in the representative volume for which the material can be treated as a continuum) is a necessary condition of fracture, but not a sufficient one. For the fracture to form, the stress must also reduce to zero, and for this to happen the energy characterizing the complete stress-strain curve must be supplied. Thus, the strength criterion indicates only whether the fracture formation can initiate, while the energy criterion indicates whether the fracture can actually form.

The standard approach to fracture analysis (21) is to calculate the rate at which the structure can release energy into the fracture front (the energy release rate) and equate it to the fracture energy (energy of fracture formation per unit crack extension). Equivalently to rates, one can equate the energies per infinitesimal crack length increment. This, however, has no direct physical meaning on a scale that is not large compared to material inhomogeneities. In this regard, it is more realistic to consider only crack length increments which exceed several aggregate sizes, i.e., to consider finite jumps in crack length. Concerning the problems of crack spacing which interest us here, the dimensions of the region in which we analyze fracture are normally less than 10–20 aggregate sizes. We therefore propose here, as an unconventional approach, to treat the formation of cracks in this region integrally, considering the entire crack to form simultaneously in one finite jump.

[1]Prof. of Civ. Engrg. and Dir., Center for Concrete and Geomaterials, Technological Inst., Northwestern Univ., Evanston, Ill. 60201.

[2]Asst. Prof., Dept. of Civ. Engrg., Technical Univ., Seoul, Korea.

Note.—Discussion open until February 1, 1984. To extend the closing date one month, a written request must be filed with the ASCE Manager of Technical and Professional Publications. The manuscript for this paper was submitted for review and possible publication on April 12, 1982. This paper is part of the *Journal of Structural Engineering*, Vol. 109, No. 9, September, 1983. ©ASCE, ISSN 0733-9445/83/0009-2066/$01.00. Paper No. 18238.

Thus, instead of considering the energy release rates, we will consider the total energies released by the structure and consumed by the formation of cracks. Note that this is not only more realistic but also more convenient, since the integral energy balance leads to algebraic equations, while the standard fracture mechanics analysis based on energy release rate leads to differential equations (21) [for a further explanation, see Appendix I of the Technical Note which follows (4)].

Note also that the strain energy released during the crack formation depends on both the states before and after the crack formation. This marks a crucial difference from the strength criterion which involves only the state before cracking.

There are now basically two possibilities for the states to be considered before and after cracking. Either we consider the formation of the first cracks, in which case there are no cracks in the initial state and the stress in concrete may be considered uniform, or we consider the formation of intermediate (secondary) cracks during further loading, by which the spacing, s, of the initially existing cracks is reduced to $s/2$. In the latter case, the stress states before and after cracking are similar and, consequently, the expressions for the energy change of the region come out simpler. At the same time, we should note that the immediate formation of a complete regular system of parallel cracks from an uncracked state is unlikely for reasons of random scatter in the values of fracture energy and other material properties. The material is weaker at some points than others, and so the very first cracks will always be only few and very far apart. Accordingly, we now restrict attention to the question when the crack spacing, $2s$, is halved, i.e., becomes s. (Some of the formulas will, nevertheless, also apply to the formation of the first cracks.)

Method of Approximate Analysis

We consider a prismatic region of concrete (Fig. 1) which contains at its axis one reinforcing bar and has a rectangular cross section of sides b_1 and b_2, denoted so that $b_1 \leq b_2$. This can serve as a model not only for a concrete member with a single reinforcing bar, but also for the situation around one bar in a row of parallel bars of spacing, b_1, in a wall [plate, shell, slab, panel (Fig. 1)], or in a rectangular array of bars. In treating all these situations in the same manner, we must abandon the conditions for compatibility of strains in the transverse direction, and we must limit consideration to only uniaxial stress in the bar direction, distributed uniformly over the region, for the sake of simplicity.

To simplify our analysis, we will further treat the prismatic region as a cylindrical region with diameter b such that the cross-sectional area, A, of the region remains the same, i.e., $A = b_1 b_2 = \pi b^2/4$ or

$$b = 2\left(\frac{A}{\pi}\right)^{1/2}; \quad A = b_1 b_2 \qquad (1)$$

To simplify the stress analysis, we will exploit the old concept of inclined "stress lines" along which a concentrated force—in our case the force transmitted into concrete by bond—spreads into an elastic solid. Referring to Fig. 1(g), we thus imagine that the formation of an intermediate crack relieves the stress within the shaded triangular regions, 012, and that the preceding cracking has already relieved the stress in the triangular regions, 456 [Fig. 1(g)]. The slope of the stress lines limiting these regions is roughly 0.7, the precise value to be determined empirically since this concept is approximate (Appendix I, Ref. 4).

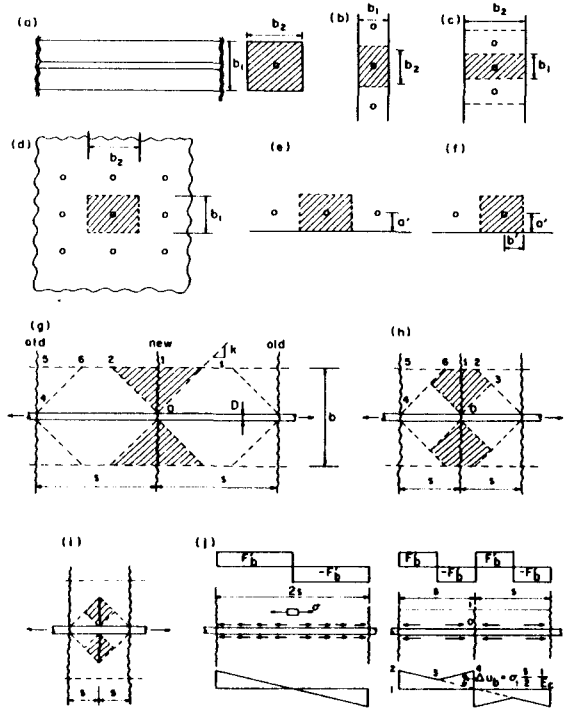

FIG. 1.—Reinforcing Bar Embedded in Concrete: (*a*) Single Bar; (*b–f*) as Part of Bar System; (*g–j*) Schematic Stress Distributions

The method of stress lines works reasonably only when the geometry of the stress relief region is simple. This includes the cases of very sparse cracks [$s >> b/2$, Fig. 1(g)] or very dense cracks [$s << b/2$, Fig. 1(i)], but not the case in Fig. 1(h) for which $s/b \approx 1$. For this situation, we will therefore have to devise a certain approximate interpolation technique.

It must be admitted that the method of stress lines is often correct only in the order of magnitude, and a two or three-fold error is possible. However, the relative error remains about the same for similar geometries, and the method gives correct structure of the expression for the energy release, except for a numerical factor. Since we will calibrate the numerical factor by test data, the method seems acceptable.

It is well known that the bond shear stresses may cause the steel bars to slip. To make explicit formulas attainable, we will assume that either there is no bond slip or the bond slip occurs over the entire length of the bar and the bond shear force per unit length, F_b, is constant and equal to its ultimate value, F_b'. In reality, F_b is of course variable; it equals

zero at intersections with the cracks and at the midlength between the cracks, causing the length L_b of bond slip to become in reality less than the crack spacing. Furthermore, the value of F'_b need not be the same as that from pullout tests. Because we deal here with a much shorter bond slip length and smaller slip displacements, F'_b can be higher than in these tests.

Do we need to consider that a transition from a no-slip situation to bond slip can occur during crack formation? Within our assumptions we do not, as long as we assume the bond slip to occur over the entire length of the bar between the cracks. We consider the crack to form at a constant overall deformation, and so the crack formation generally relieves the stresses. After the crack spacing is halved, the situation is geometrically similar and stress distribution is then also similar for our assumptions. Thus, if there is no bond slip before cracking, there is none after cracking in our model. An exception is the formation of first cracks during which the bond slip can occur. Although it would be possible to analyze this case with our method, we omit it for the reasons already explained.

Conditions for Initiation of Microcrack Bands.—If there is no bond slip, the strength criterion requires that

$$\epsilon_s \geq \frac{f'_t}{E_c} \quad \text{(no slip)} \qquad (2)$$

in which f'_t = tensile strength of concrete; and E_c = its Young's modulus. (This condition also applies to the formation of first cracks.)

If there is bond slip, the cracks initiate only if the stress produced in segment 01 [Fig. 1(*g*,*i*)] by the bond force accumulated over the bond slip length, L_b, equals f'_t. We now distinguish the case of very sparse cracks ($s \gg b/2$) and very dense cracks ($s \ll b/2$). For $s \gg b/2$ [Fig. 1(*g*)], the equilibrium condition is $F'_b L_b = \pi(b^2 - D^2)f'_t/4$, and since $L_b \leq s$, we may write for $s >> b/2$:

$$s \geq \frac{\pi f'_t}{F'_b h_1}; \quad h_1 = \frac{4}{b^2 - D^2} \qquad (3)$$

For $s << b/2$ [Fig. 1(*i*)], the equilibrium condition is $F'_b L_b = \pi[(2ks + D)^2 - D^2]f'_t/4$, and since $L_b \leq s$ we get for $s << b/2$:

$$s \geq \frac{\pi f'_t}{F'_b g_1(s)}; \quad g_1(s) = \frac{1}{ks(ks + D)} \qquad (4)$$

For any s/b we may now expect, upon comparing Eqs. 3–4, that $s \geq \pi f'_t/F'_b \phi_1(s)$, in which $\phi_1(s)$ = a smooth function which approaches h_1 when $s >> b/2$, and $g_1(s)$ when $s << b/2$ [Fig. 2(*a*)]. A simple function which has these two asymptotic properties is $\phi_1(s) = h_1 + g_1(s)$, and with it we acquire the general approximate relation

$$\frac{4s}{b^2 - D^2} + \frac{1}{k(ks + D)} \geq \frac{\pi f'_t}{F'_b} \quad \text{(bond slip)} \qquad (5)$$

which we now need to solve for s. We may transform Eq. 5 into the quadratic inequality $s^2 + 2p_1 s + p_2 \geq 0$, in which

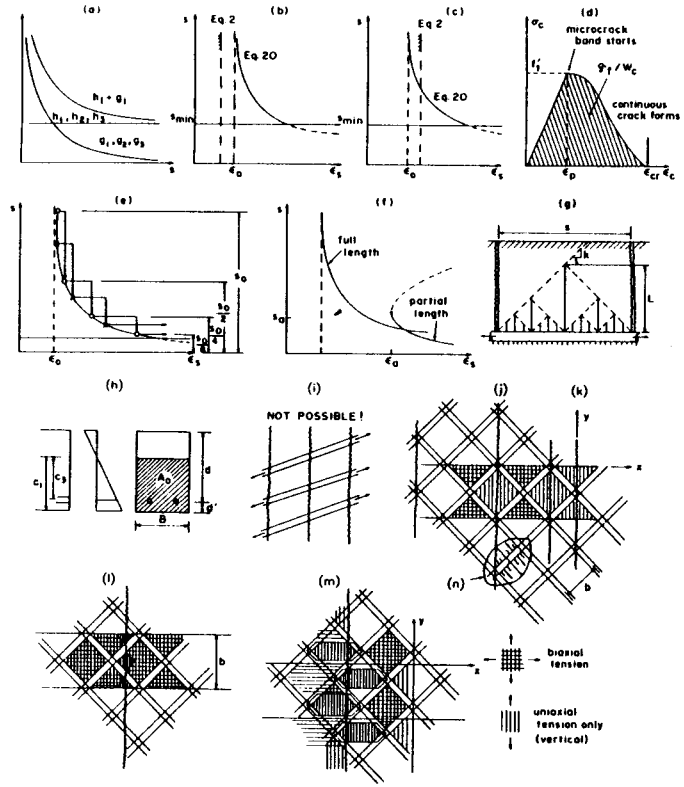

FIG. 2.—(*a*) Auxiliary Functions; (*b,c,e,f*) Spacing-Strain Diagrams; (*d*) Stress-Strain Diagram; (*g*) Cracks of Partial Length; (*h*) Interacting Concrete Area for Bending; (*i–n*) Parallel Crack Systems Skew to Bars

$$p_1 = \frac{D}{2k} - \frac{\pi f'_t}{8F'_b}(b^2 - D^2); \quad p_2 = \frac{b^2 - D^2}{4k}\left(1 - \frac{\pi f'_t kD}{F'_b}\right) \qquad (6)$$

Denoting $s_{1,2} = -p_1 \pm (p_1^2 - p_2)^{1/2}$ (the roots), we may write this inequality as $(s - s_1)(s - s_2) \geq 0$. The solution then is

$$s \geq s_1 \quad \text{or} \quad (\text{if } s_2 > 0)\ s \leq s_2 \quad \text{(bond slip)} \qquad (7)$$

We see that the strength criterion provides a lower bound, s_1, on the crack spacing at which cracks can initiate if there is bond slip. However, there may also exist an upper bound, s_2, above which no regularly spaced cracks can exist.

Eqs. 2 and 7 indicate whether the microcracking can start but not whether it can lead to the formation of a distinct crack. This question is decided by the energy criterion, to which we turn our attention now.

Energy Approximations and Conditions for Continuous Crack Formation.—Consider first that there is no bond slip. If the cracks are sparse ($s >> b/2$), the stress relief region is a body of revolution whose cross

section is crosshatched as in Fig. 1(*g*); its volume is $V = \pi(b - D)^2(2b + D)/24k$. Since there is no bond slip, the strain energy density in this volume before cracking is $E\epsilon_s^2/2$. So, the energy release due to the formation of the intermediate cracks is $\Delta U = VE_c\epsilon_s^2/2$ or for $s >> b/2$:

$$\Delta U = \frac{E_c\epsilon_s^2}{2h_2}; \quad h_2 = \frac{24k}{\pi(b - D)^2(2b + D)} \quad \text{(no slip)} \quad (8)$$

If the cracks are dense ($s << b/2$), the stress relief region is a body of revolution whose cross section is crosshatched as in Fig. 1(*i*); its volume is $V = 2\pi(ks + D)ks^2/8$, and since $\Delta U = VE_c\epsilon_s^2/2$ for $s << b/2$:

$$\Delta U = \frac{E_c\epsilon_s^2}{2g_2(s)}; \quad g_2(s) = \frac{4}{\pi ks^2(ks + D)} \quad \text{(no slip)} \quad (9)$$

Comparing Eqs. 8–9, we may now expect that for any s/b, $\Delta U = E_c\epsilon_s^2/2\phi_2(s)$, in which $\phi_2(s)$ = a smooth function which asymptotically approaches h_2 when $s >> b/2$, and $g_2(s)$ when $s << b/2$ [Fig. 2(*a*)]. A simple function which has these two asymptotic properties is $\phi_2(s) = [h_2^n + g_2(s)^n]^{1/n}$. (From test data fitting, the value $n = 4$ was found to be reasonable.) Thus, for any s/b

$$\Delta U = \frac{V}{2}E_c\epsilon_s^2; \quad V = \left[\left(\frac{24k}{\pi(b - D)^2(2b + D)}\right)^n + \left(\frac{4}{\pi ks^2(ks + D)}\right)^n\right]^{-1/n} \quad \text{(no slip)} \quad (10)$$

is obtained.

Suppose now that the steel bars slip. The stress, σ_1, in concrete in the crosshatched regions of Fig. 1(*g, i*) before cracking no longer is $E_c\epsilon_s$ and must be figured out from the ultimate bond forces, F_b', applied on concrete along the bar [Fig. 1(*j*)]. Their resultant is $F_b's$, and so the average stress on the cross section, 01, in Fig. 1(*j*) or Fig. 1(*g, i*) is, approximately, for $s >> b/2$:

$$\sigma_1 = F_b's\,h_3; \quad h_3 = \frac{4}{\pi(b^2 - D^2)} \quad (11)$$

For $s << b/2$, we consider the average σ_1 at distance $s/2$ from the crack:

$$\sigma_1 = F_b's\,g_3(s); \quad g_3(s) = \frac{1}{\pi ks(ks + D)} \quad (12)$$

Here $1/h_3$ and $1/g_3(s)$ represent the cross-sectional areas [Fig. 1(*g, i*)] over which σ_1 is distributed. Comparing Eqs. 11–12, we may now expect that, for any s/b, $\sigma_1 \simeq F_b's\phi_3(s)$, in which $\phi_3(s)$ = a smooth function which asymptotically approaches h_3 when $s >> b/2$, and $g_3(s)$ when $s << b/2$ [Fig. 2(*a*)]. A simple function which exhibits these two asymptotic properties is $\phi_3(s) = h_3 + g_3(s)$; this yields, for any s/b, $\sigma_1 = F_b's[h_3 + g_3(s)]$ or

$$\sigma_1 = \frac{F_b's}{\pi}\left[\frac{4}{b^2 - D^2} + \frac{1}{ks(ks + D)}\right] \quad (13)$$

The loss of strain energy due to crack formation may now be expressed for any s/b as

$$\Delta U = \frac{V}{2E_c}\sigma_1^2 \quad \text{(bond slip)} \quad (14)$$

in which V = the same as already given in Eqs. 10.

The work, ΔW_f, consumed by fracture formation depends on the crack area. If the crack spacing is not sufficiently sparse, the cracks do not extend all the way to the boundary of the region. According to the inclined stress lines indicating the spread of the bond force [Fig. 1(*i*)], this occurs when $ks + D/2 < b/2$. Thus, for $s \le b - D/2k$:

$$\Delta W_f = \pi ks(ks + D)\mathcal{G}_f \quad \text{(short cracks)} \quad (15)$$

If $ks + D/2 \ge b/2$, the crack cuts all the way across the width, b, and we have for $s \ge b - D/2k$:

$$\Delta W_f = \frac{\pi}{4}(b^2 - D^2)\mathcal{G}_f \quad \text{(full length)} \quad (16)$$

The condition for the formation of continuous cracks can now be stated as follows:

$$\Delta U \ge \Delta W_f + \Delta W_b \quad (17)$$

in which $\Delta W_b = 0$ if there is no bond slip. The case = corresponds to static (slow) crack formation, and the case > to dynamic crack formation in which the excess of the released strain energy goes into kinetic energy.

In the energy balance during crack formation, we should not forget to subtract the work consumed by a change, Δu_b, in bond slip, if any. It may be expressed as $\Delta W_b = F_b's\Delta u_b$ in which Δu_b = average change of slip. To estimate Δu_b, we sketch in Fig. 1(*j*) the distributions of the bond force, F_b, and of the strains in concrete in the vicinity of the steel bar before and after crack formation. Since ϵ_s is assumed to remain constant during the crack formation, we may consider [according to Fig. 1(*j*)] that $\Delta u_b = (\sigma_1/E_c)s/2$ in which σ_1 has already been calculated in Eq. 13. So we have, for any s/b

$$\Delta W_b = F_b'\frac{\sigma_1}{E_c}\frac{s^2}{2} \quad \text{(bond slip, full length)} \quad (18)$$

The foregoing equation gives an acceptable estimate for ΔW_b only when the cracks are of full length. In the case of partial length, σ_1 varies within the region and the value of σ_1 at the line of symmetry is not a good approximation for σ_1. ΔW_b may be expressed as $\Delta W_b = F_b'\int \Delta u_b dx$ in which Δu_b = bond slip change from before cracking to after cracking [Fig. 1(*j*)]. Before cracking, $F_b'\int u_b dx$ must equal ΔU given by Eq. 14 due to the requirement of energy conservation in the region of stressed concrete (considered elastic). From Fig. 1(*j*) we see that $F_b'\int \Delta u_b dx = (1/2)F_b'\int u_b dx$ and, therefore, $\Delta W_b = \Delta U/2$ in which ΔU is given by Eq. 14. So we have

$$\Delta U = \Delta W_b = \frac{V}{4E_c}\sigma_1^2 \quad \text{(bond slip, short cracks)} \quad (19)$$

Approximate Relation of Crack Spacing to Strain.—As the strain is increased, the first cracks appear at a certain strain and subsequently further cracks are produced, which causes the crack spacing to diminish as the strain grows. We are therefore interested in constructing the diagram of s vs. ϵ_s. At the beginning of loading the cracks may be supposed to be far apart and no bond slip to exist. The energy requirement for fracture to occur is that $\Delta U \geq \Delta W_f$ in which ΔW_f is given by Eq. 16. This yields, for the cracks cutting all the way across the width, b:

$$\epsilon_s = \left[(\epsilon_0^2)^n + \left(\frac{2\mathcal{G}_f}{E_c} \frac{b^2 - D^2}{ks^2(ks + D)} \right)^n \right]^{1/2n} \quad \text{(no slip, full length)} \quad \ldots\ldots\ldots (20)$$

$$\text{in which} \quad \epsilon_0 = \left(\frac{12\mathcal{G}_f}{E_c} \frac{k(b + D)}{(b - D)(2b + D)} \right)^{1/2} \quad \ldots\ldots\ldots (21)$$

A typical plot of Eq. 20 is shown in Fig. 2(b,c). The value ϵ_0 represents the minimum strain which the energy criterion requires for the formation of any complete cracks. At $\epsilon_s < \epsilon_0$ we can have only microcrack bands but no complete cracks, and at $\epsilon_s = \epsilon_0$ complete cracks begin to form at spacing $s \to \infty$.

Eq. 20 must now be compared with the strength condition for the microcrack band initiation: $\epsilon_s \geq f_t'/E_c$ (Eq. 2). If this value is less than Eq. 20 gives, Eq. 20 governs, and cracks form gradually, i.e., microcracking progresses at increasing strain and decreasing stress until continuous cracks form. If Eq. 2 gives a larger value than Eq. 20, then we must use

$$\epsilon_s = \max \quad \text{(Eq. 20, Eq. 2)} \quad \ldots\ldots\ldots (22)$$

in which Eq. 2 prevails until a certain strain value, and then afterwards Eq. 20 prevails. In the cases where Eq. 2 prevails, the cracks form suddenly, with a snap (dynamic process), since the excess of ΔU over ΔW_f must go into kinetic energy [Fig. 2(b–d)].

At a certain, sufficiently large strain, the bond strength becomes exhausted and the bars slip within concrete. Considering cracks of full length, we now have ΔU given by Eqs. 13–14, ΔW_f by Eq. 16, and ΔW_b by Eq. 18. Eq. 17 then yields the condition

$$F(s) = \frac{V\sigma_1^2}{2E_c} - \frac{F_b' s^2}{2E_c}\sigma_1 - \frac{\pi}{4}(b^2 - D^2)\mathcal{G}_f \geq 0 \quad \text{(full length)} \quad \ldots\ldots\ldots (23)$$

This condition does not involve ϵ_s, and so the solution is a fixed lower limit on the spacing of the cracks of full length [$s_{\min}$ in Fig. 2(b,c)]. The left-hand side of Eq. 23 has the form $P(s)/s^3$ in which $P(s)$ = a sixth-order polynomial in s. The solution of Eq. 23 can be obtained by Newton iteration.

An approximation to the solution of Eq. 23 can, however, be obtained by replacing Eq. 13 with the limiting value for sparse cracks, $\sigma_1 \simeq 4F_b' s/\pi(b^2 - D^2)$, and Eqs. 10 with $V \simeq \pi(b - D)^2(2b + D)/24k$, and by neglecting ΔW_b, then

$$s_{\min} = \left(\frac{3\pi^2 k E_c \mathcal{G}_f (b - D)(b + D)^3}{4F_b'^2(2b + D)} \right)^{1/2} \quad \text{(full length)} \quad \ldots\ldots\ldots (24)$$

If we want to calculate s from Eq. 20, we need to solve a cubic equation. An approximate solution may be obtained by neglecting D, and we then get

$$s \geq \left(\frac{8\mathcal{G}_f A}{\pi k^2 E_c [(\epsilon_s^2)^n - (\epsilon_0^2)^n]^{1/n}} \right)^{1/3}; \quad \epsilon_0^2 = \frac{6k\mathcal{G}_f}{E_c b} \quad \ldots\ldots\ldots (25)$$

in which $A = \pi b^2/4$. When the ratio ϵ_s/ϵ_0 is large, the ϵ_0 value may be neglected, of course, compared to ϵ_s, and then s is proportional to $\sqrt[3]{A}$. This observation is interesting with regard to the well-known work of Gergely and Lutz (16,23). Using extensive statistical curve-fitting analysis of numerous test data rather than a mechanical analysis, they found that the crack width, w, is about proportional to $\sqrt[3]{A}$. Since w is roughly proportional to s (see Eq. 32 in the sequel), Eqs. 25 now give theoretical support to Gergely and Lutz's important classical result. This result, in turn, reinforces our theoretical arguments.

The continuous relation between s and ϵ_s that we established (Eq. 20) does not mean that the crack spacing, s, varies continuously as the strain increases. This relation merely indicates the successive strain values at which the existing crack spacing is halved by the formation of intermediate cracks. The evolution of the crack system by successive halvings of its spacing is depicted by the descending staircase in Fig. 2(e), for which the bottom corners of the steps lie on the smooth curve of s versus ϵ_s. Because $s \to \infty$ at $\epsilon_s \to \epsilon_0$, the magnitude of the initial spacing can scatter very greatly with only small deviations from ϵ_0. Therefore, the value of the initial spacing is essentially random, and for any point on the smooth (s,ϵ_s) curve there always exists an initial state (with strain as close to ϵ_0 as desired) from which this point can be reached by successive halvings.

The foregoing solutions apply only for cracks of full length, cutting all across the width b. For short cracks (i.e., those of length less than b), different relations ensue. Consider first that the bars do not slip. Then, setting $\Delta U \geq \Delta W_f$ and substituting Eqs. 10 and 15, we find that the strain must equal or exceed the values for $s \leq b - D/2k$:

$$\epsilon_s = \left\{ \left(\frac{8k\mathcal{G}_f}{E_c} \right)^n \left[\left(\frac{6ks(ks + D)}{(b - D)^2(2b + D)} \right)^n + \left(\frac{1}{ks} \right)^n \right] \right\}^{1/2n} \quad \text{(short cracks, no slip)} \quad \ldots\ldots\ldots (26)$$

in which $n \simeq 4$ is most reasonable. This equation is plotted in Fig. 2(f). We may note that for a given ϵ_s value there may exist two possible values of s when $\epsilon_s > \epsilon_a$, and none when $\epsilon_s < \epsilon_a$, in which ϵ_a [Fig. 2(f)] is obtained by setting $\partial\epsilon_s/\partial s = 0$. The solution is simple only when $n = 1$ [Fig. 2(f)], and then we obtain a cubic equation for the corresponding value, s_a. Furthermore, when also $D/b << 1$, Eq. 26 simplifies to

$$\epsilon_s = \left[\frac{8\mathcal{G}_f}{E_c} \left(\frac{3k^3 s^2}{b^3} + \frac{1}{s} \right) \right]^{1/2} \quad \text{(for } D << b, n = 1) \quad \ldots\ldots\ldots (27)$$

The condition, $\partial\epsilon_s/\partial s = 0$, then yields for s and ϵ the solutions

$$s_a = 0.550\frac{b}{k}; \quad \epsilon_a = \left(\frac{21.8k\,\mathcal{G}_f}{b\,E_a}\right)^{1/2} \quad (\text{for } D << b,\ n = 1) \ldots\ldots\ldots\ldots (28)$$

Now we may note that the limitation $s \leq b/2k$ ($D \simeq 0$) is stricter than $s \leq 0.550\ b/k$. Therefore, the upper branch shown as the dashed portion in Fig. 2(f) never applies, and the same may be supposed to approximately hold for finite D.

As mentioned before, the length, L, of these short cracks when they form cannot exceed a certain limit (approximately $L \leq ks/2$, in which $k \simeq 0.7$). Thus, as long as the bond slip does not occur, the pattern of cracks produced by successive halvings of the spacing as the strain increases looks like that shown in Fig. 2(g). The intermediate cracks are getting shorter and shorter and the cracks are getting denser and denser. This type of behavior, as sketched in Fig. 2(g), was experimentally observed by Broms (11,12) in his study of bending cracks in beams. A fundamental theoretical explanation, with exact rules, governing this behavior was obtained through stability analysis of parallel crack systems (6,10).

Suppose now that the bar slips; for simplicity consider the case $s << b/2$. Then, substituting Eq. 15 and Eq. 19 with σ_1 according to Eqs. 12, and with $V = \pi ks^2\,(ks + D)/4$ into Eq. 17, we obtain

$$s \leq s_0 = \frac{F_b'^2}{16\pi^2 k^4 E_c \mathcal{G}_f} \ldots\ldots\ldots\ldots (29)$$

which represents the upper bound on possible crack spacing for short cracks. In the case where this bound is smaller than the bound in Eq. 23 for full-length cracks, cracks of partial length can never form. In the opposite case, they will.

The bound, s_0 (Eq. 29), must be compared further with the strength bound, s_2, in Eq. 7. If $s_2 < s_0$, then the strength criterion governs and the bound, s_0, in Eq. 7 can never be reached.

Crack Opening Width.—If the concrete between the cracks were without stress, then the crack opening width would be $w = s\epsilon_s$. Due to the tensile straining of concrete, this is merely an upper bound, i.e., $w \leq s\epsilon_s$. To estimate w, we must now subtract from $s\epsilon_s$ the deformation due to the tensile stress in concrete. For the crack width near the surface of the bars, we may thus write

$$w \simeq s\epsilon_s - s\frac{\sigma_1}{E_c} \quad (\text{near bars}) \ldots\ldots\ldots\ldots (30)$$

Here σ_1 is given by Eq. 13 if there is bond slip. If there is no bond slip, we have $w = 0$ at the bar surface. (This is due to our assumptions; in reality, there will always be some bond slip and crack opening even at bond forces less than F_b'.)

For the crack width at the boundary of the region of width b, stress σ_1 exists only over a portion of the distance between the cracks, and over the remaining portion the axial stress is assumed zero. Thus, we may write for $s \geq b - D/k$:

$$w = s\epsilon_s - \left(s - \frac{b - D}{k}\right)\frac{\sigma_1}{E_c} \ldots\ldots\ldots\ldots (31)$$

and for $s \leq b - D/k$:

$$w = s\epsilon_s \ldots\ldots\ldots\ldots (32)$$

Numerical Example.—To illustrate our formulation, consider the following example: $b = 4$ in. (10.16 cm); $D = 0.75$ in. (1.905 cm); $E_s = 29 \times 10^6$ psi (200,000 MPa); $E_c = 3 \times 10^6$ psi (20,690 MPa); $f_t' = 400$ psi (2.758 MPa); and $k = 0.7$. We estimate the fracture energy from a new formula, $\mathcal{G}_f = (2.72 + 0.0214\,f_t')\,f_t'^2 d_a/E_c$ (developed in Ref. 3), in which d_a = maximum aggregate size. Considering $d_a = 1$ in., we thus have $\mathcal{G}_f = 0.602$ lb/in. (105.3 N/m). The calculated results for crack spacing and crack width are shown in Fig. 3(a,b). The values of the crack spacing are obtained by solving Eqs. 10 and 16 for the full-length cracks. The minimum crack spacing expressed by Eq. 24 is shown by the dash-dot line in Fig. 3(a). The lower value of the minimum crack spacing can be obtained by using a larger bond force [see the dash-dot line at bottom of Fig. 3(a)]. The crack width is calculated from Eqs. 31–32 and is shown in Fig. 3(b).

Now we consider the case when $b = 6$ in. (15.24 cm), with the other data remaining the same. The calculated curves for this case are shown in Fig. 3(c,d) in the same manner as in Fig. 3(a,b).

Extension to Beams in Flexure.—Although we assumed the initial stress before cracking to be uniform, we may apply our formulation in an approximate sense also to situations where the initial stress is nonuniform. This is the case in beams under flexure [Fig. 2(h)]. To find an equivalent situation within our assumptions, it is perhaps best to assume that the strain energy of concrete within area A_0 below the neutral axis [Fig. 2(h)] is equal to the strain energy within an equivalent area, A_e, in which the strain is uniform and the same as the actual steel strain. This requirement yields $\int_0^0 E_c\epsilon^2 B dz/2 = E_c\epsilon_s^2 Bb/2$, in which B = beam width, b = the depth of equivalent area A_e [Fig. 2(h)], ϵ = actual strains due to bending, and z = a coordinate. Since $\epsilon = \epsilon_s z/c_3$, we obtain

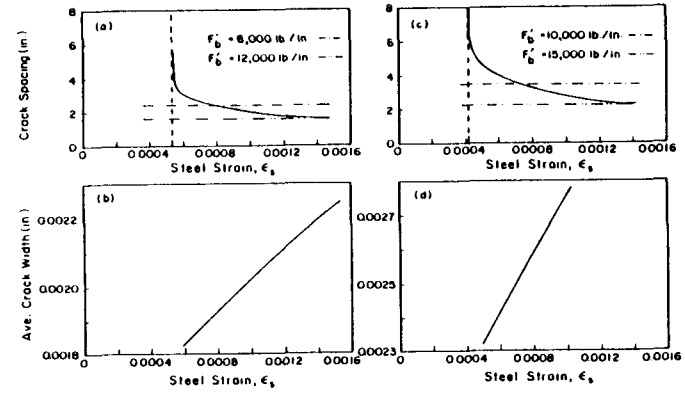

FIG. 3.—Diagrams of Spacing or Crack Width versus Strain Calculated from Typical Numerical Examples (1 in. = 25.4 mm)

$$b = \frac{c_1^3}{3c_3^2} \quad \text{(33)}$$

in which c_1, c_3 = distances from the neutral axis to the bottom face and to the steel bar axis. This value of b may then be used in the preceding formulation, considering the bar to be in the center of depth b.

Comparison with Test Data

To verify our formulation, we show in Figs. 4–6 comparisons with the test data available in the literature (13,14,18–20,22). The parameters of our formulation which correspond to the plotted curves are listed in Table 1. For all the figures, $k = 0.7$ was used as it was found to give the best results.

In our comparisons with the test data, we must be cautious in interpreting the observed crack spacing. For a regularly spaced crack system, the crack spacing may decrease with increasing strain only by halvings, but the reported data (13,14) indicate a series of much smaller decreases in the crack spacing (Fig. 4). This is due to the fact that the observed crack system was no doubt somewhat irregularly spaced, and that the overall bar extension was not the same between each two cracks (due

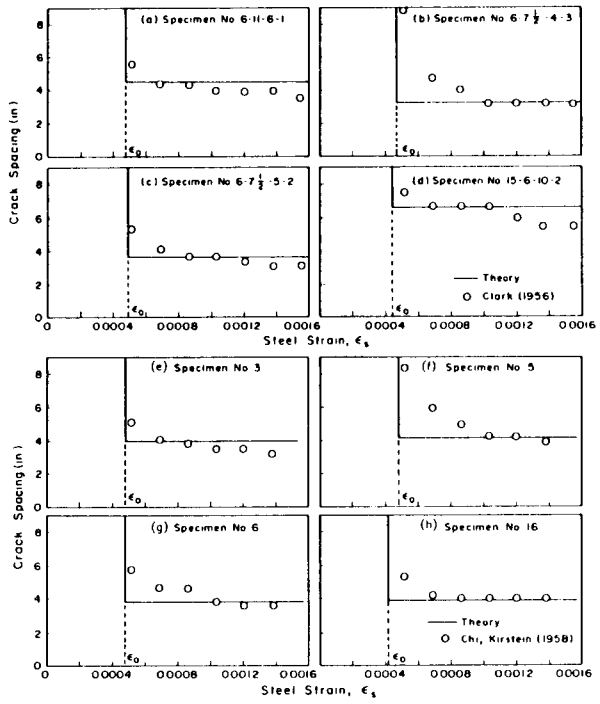

FIG. 4.—Comparison of Calculated Crack Spacing with Test Data by: (*a–d*) Clark (1956); (*e–h*) Chi and Kirstein (1958)

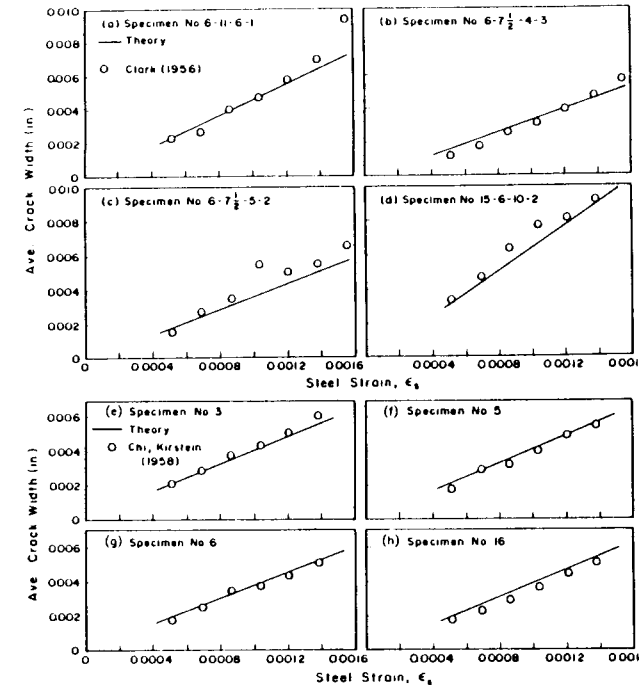

FIG. 5.—Comparison of Calculated Average Crack Width with Test Data by: (*a–d*) Clark (1956); (*e–h*) Chi and Kirstein (1958)

to variation of the bending stress along the beam near its ends). Such irregularities, although inevitable, are not covered by our theory. Since the overall observed decrease of crack spacing is less than one half, it would make no sense to use our formula for the s vs. ϵ_s curve (Eqs. 20, 21, 25), and so we must content ourselves by fitting the test data in Fig. 4 (14,13) merely with the formula for the constant limiting (minimum) values of crack spacing (Eq. 24). The corresponding crack widths may be calculated by using Eqs. 31–32. A possible effect of transverse reinforcement, which we neglect, may also cause deviations from our theory.

Fig. 4 shows the comparisons of our theory for the crack spacing with the test data by Clark (14), and Chi and Kirstein (13). Fig. 5(*a–d*) shows a comparison with the average crack width data by Clark, indicating an increase of crack width with the increase of steel strain. Fig. 5(*e–h*) shows crack width comparisons for the data by Chi and Kirstein. Fig. 6 shows the comparisons with similar data by Kaar and Mattock (20), Hognestad (18), and Mathey and Watstein (22).

We see that despite various rather crude approximations, our theory compares satisfactorily with test data and better than the previously developed empirical formulas. Since our theory was developed theoretically, it should also have broader applicability, i.e., it should be applicable even for cases outside the range of existing test data.

Statistical Analysis of Errors and Prediction of Material Parame-

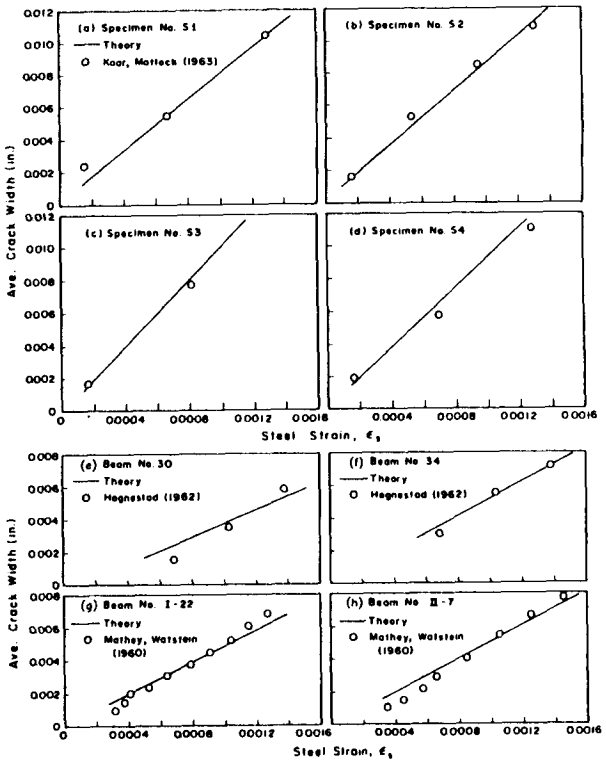

FIG. 6.—Comparison of Calculated Average Crack Width with Test Data by: (*a–d*) Kaar and Mattock (1963); (*e,f*) Hognestad (1962); (*g,h*) Mathey and Watstein (1960)

ters.—To determine statistical characteristics of errors in the crack width, we may construct the plot of $Y = w_m$ vs. $X = w_t$ in which w_m = measured crack width, and w_t = theoretical crack width. This plot, based on n = 88 data points taken from Figs. 5–6, is shown in Fig. 7(*a*). If the material behaved deterministically, and if our theory were perfect, the plot would have to be a straight line $Y = a + bX$ with $a = 0$, $b = 1$. So, a linear regression analysis may be applied. The difference of a from 0 and of b from 1 then indicates possible improvement in the optimum calibration of our theory [which is seen to be negligible for Fig. 7(*a*)]. The errors, i.e., the vertical deviations of data points, Y_i, from the regression line, $Y' = a + bX$, indicate how good the theory is. The coefficient of variation of the errors, defined as $\omega = s/\bar{Y}$, in which s = standard error, $s^2 = \Sigma(Y_i - Y')^2/(n-2)$, and $\bar{Y} = \Sigma\, Y_i/n$ ($i = 1, 2, \ldots, n$), is found to be ω = 0.120.

Another useful plot may be constructed by plotting $Y = w_m/\epsilon_s$ vs. $X = w_t/\epsilon_s$ in which ϵ_s = steel strain [Fig. 7(*b*)]. The coefficient of variation of errors in this type of regression is found to be $\omega = 0.126$.

The 95% confidence limits corresponding to ω are plotted as the dashed curves in Fig. 7(*a,b*). These curves are hyperbolas, but due to the large

TABLE 1.—Parameters for Test Data

Test Series (1)	E_c, in thousand pounds per square inch (2)	$\mathcal{G}_f$, in pounds per inch (3)	f'_c, in pounds per square inch (4)	d_a, in inches (5)	F'_b, in pounds per inch (6)	F^*_b, in pounds per inch (7)
1. Clark	No. 1 3,212	0.505	385	1.0	3,876	3,895
	2 3,192	0.411	357	1.0	3,499	3,619
	3 3,457	0.412	367	1.0	3,199	3,040
	4 1,912	0.393	290	1.0	3,783	3,743
2. Chi, Kirstein	No. 1 4,277	0.684	476	1.0	5,950	5,805
	2 3,713	0.661	447	1.0	6,426	6,299
	3 3,422	0.611	422	1.0	6,391	6,322
	4 1,500	0.204	207	1.0	2,771	2,328
3. Kaar, Mattock	No. 1 2,891	0.287	259	1.5	3,470	3,819
	2 3,149	0.304	273	1.5	3,504	3,676
	3 3,028	0.524	329	1.5	3,868	4,189
	4 3,120	0.217	240	1.5	3,735	3,885
4. Hognestad	No. 1 2,514	0.109	170	1.5	2,830	2,888
	2 3,312	0.328	286	1.5	4,173	4,142
5. Mathey, Watstein	No. 1 3,246	0.251	299	1.0	3,226	3,344
	2 3,272	0.259	303	1.0	3,187	3,287

Note: psi = 6,895 N/m²; lb/in. = 175.1 N/m; in. = 25.4 mm; ksi = 1,000 psi. All numbers except d_a had to be estimated, in order to get optimum fit, because they were not reported by the experimentalists.

size of our statistical samples they are almost straight, in which case the 95% confidence limits relative to mean $\bar{Y}$ are approximately 1.96 ω.

We see from Fig. 7 that our theory achieves a satisfactory agreement with test data.

As for the errors in the crack spacing, we may characterize them by the coefficient of variation, ω_s, of the population of the values of s_m/s_t, s_m and s_t being the measured and theoretical spacings. From all the data points in Fig. 4 we get $\omega_s = 0.145$. We should note, however, that a statistical comparison of the errors in spacing based on Fig. 4 is of limited relevance since, as we mentioned before, the spacing data available involve some irregular spacings, do not have a sufficient range to show the halving of spacing, and do not permit showing the changes of regular spacing with steel strain. Because of probable irregular spacing, the first and the last data points in Fig. 4 were not included in the calculation of ω_s given previously.

To calculate the fracture energy, $\mathcal{G}_f$, the recently developed new formula from Ref. 3 has been used.

The values of ultimate bond force, F'_b, obtained as the optima for fitting the data (Table 1) may be analyzed to see whether they show some systematic pattern and can be approximately predicted. Assuming that F'_b depends on the compressive strength, f'_c, of concrete, and carrying out a least-square regression analysis of the optimum values of F'_b listed in Table 1, we can obtain the following approximate formula for the ultimate bond force per unit length of a deformed steel bar:

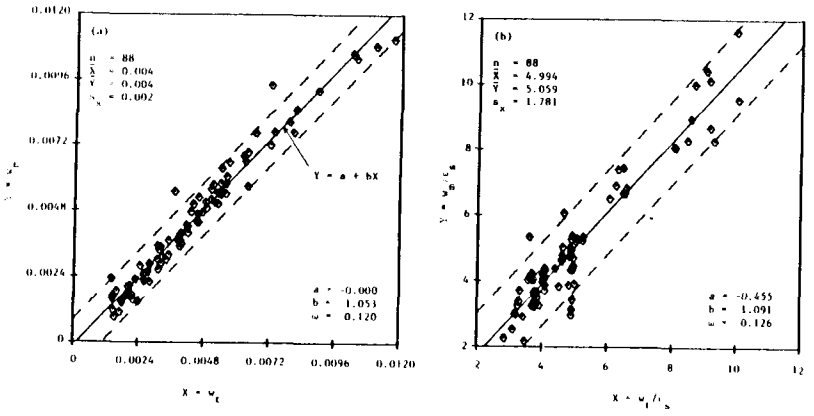

FIG. 7.—Plot of Measured versus Theoretical Values for Crack Width Based on Figs. 5–6

$$F_b^* = 0.95 f_c' \quad \text{(34)}$$

in which F_b^* = predicted value of F_b', f_c' must be in psi, and F_b^* is in lb/in. (1 psi = 6,895 Pa, 1 lb/in. = 175.1 N/m). Note that the values of F_b^* and F_b' are generally larger (roughly by 70%) than the usual bond force, U_b', determined by pullout tests and used in determining the development length of steel bars. This is because we deal here with a localized bond slip occurring only over a short bar length.

For all 16 data sets listed in Table 1, the errors of Eq. 34, i.e., $F_b^* - F_b'$ (with F_b^* and F_b' listed in Table 1), have the coefficient of variation ω_f = 0.051, which seems acceptable.

Formation of Skew Cracks.—General loading can produce a system of parallel cracks which are not normal to the reinforcing bars. A uniaxial applied stress in the bar direction will obviously always produce cracks normal to the bars, and so the skew cracks can only be produced under multiaxial applied stress, in which case the reinforcement would normally be designed as an orthogonal mesh rather than a system of parallel bars.

Consider an orthogonal regular reinforcing net with identical bar spacings and diameters for bars of both direction [Fig. 2(*i–n*)]. Suppose that the cracks form at angle 45° with the bars [Fig. 2(*i–n*)]. To produce such cracks, the axial strains in the bars of both directions must be the same. Before the first cracking, the concrete would be roughly in a state of biaxial tension, $\sigma_x = \sigma_y$. Formation of a crack in y-direction would relieve some of the stress, σ_x, but would have no effect on c_y. Applying again the method of inclined stress lines (with $k = 1$), we may consider that the formation of vertical cracks in Fig. 2(*j–l*) would relieve stress, σ_x, from the vertically crosshatched triangular regions and would have no effect on the stress in the remaining regions.

We may now compare two possible crack locations: the cracks running through the bar crossings [Fig. 2(*j*)], and the cracks running in the middle between these crossings [Fig. 2(*l,m*)]. Comparing the areas of the

regions of relief of σ_x for both cases (vertically crosshatched regions), we see that their area is somewhat smaller for the second of these two cases [Fig. 2(*l,m*)]. Therefore, the strain energy release, ΔU, for cracks running through the bar crossings appears to be larger, and so this is the type of cracks which should form [Fig. 2(*j,k*)]. This now restricts the possible spacings to $s = nb/\sqrt{2}$ in which n = 1, 2, 3, ... We note however that ΔU per crack is the same for all these crack spacings.

Therefore, cracks of the densest spacing [Fig. 2(*k*)]:

$$s = \frac{b}{\sqrt{2}} \quad \text{(35)}$$

should form immediately when the minimum necessary axial strain, ϵ_s, in the bars is reached. For this spacing, the stress, σ_x, is completely relieved from all concrete [see the vertically shaded areas in Fig. 2(*k*)], and so $\Delta U = (E_c \epsilon_x^2/2) s b \sqrt{2} b_2$ per mesh of bars, in which b_2 = thickness of the plate. As for bond slip, none can occur before the first cracking (since the stress is uniform). Assuming that no bond slip occurs during cracking, the consumed energy is $\Delta W_f = b\sqrt{2} b_2 \mathcal{G}_f$, and setting $\Delta U = \Delta W_f$ we get

$$\epsilon_s = 1.68 \sqrt{\frac{\mathcal{G}_f}{E_c b}} \quad \text{(no slip)} \quad \text{(36)}$$

If there is bond slip, then $\Delta W_b > 0$, and so a larger strain is required to produce these cracks.

Subsequent increase of strain cannot, according to our analysis, produce further continuous skew cracks. It can, however, produce shorter, discontinuous cracks of the type already analyzed [Fig. 2(*n*)]. These are likely not to be parallel to the continuous cracks.

There are many more interesting questions with regard to skew cracks under biaxial stress, but they are beyond the scope of this study.

Summary and Conclusions

The spacing and width of cracks in a parallel crack system is approximately analyzed using the energy criterion of fracture mechanics as well as the strength criterion. Following previous works on rocks (8,10), the energy criterion is applied here in a novel way—integrally, considering the formation of the entire crack as one event. For cracks that are not long enough compared to the aggregate size, this approach appears to be more realistic than the usual fracture analysis which pertains to energy balance at infinitesimal crack length increments (i.e., balance of energy release and consumption rates). The energy criterion involves not only the release of strain energy and the energy consumed to produce the crack, but also the energy consumed by bond slip during cracking (if any).

The energy criterion indicates that the crack spacing is a function of the axial strain of the bars and also depends on bar spacing, bar diameter, fracture energy of concrete, and its elastic modulus. Both the energy and strength criteria yield a minimum strain necessary to pro-

duce any cracks. The energy criterion and the bond slip conditions also yield a lower bound on possible spacing of continuous cracks. The rules for the formation of shorter, partial length cracks are also set up. Approximate expressions for the crack width at, and away, from the bars are derived.

Numerical comparisons indicate satisfactory agreement with existing test data, and also lend theoretical support to one aspect of the empirical Gergely-Lutz formula previously obtained by statistical regression analysis of test data. Finally, formation of skew cracks in a biaxially stressed and biaxially reinforced plate is analyzed and a crack spacing formula is derived for one typical case.

Acknowledgment

Financial support under U.S. National Science Foundation Grant No. CEE8009050 to Northwestern University is gratefully acknowledged. Mary Hill is to be thanked for her excellent secretarial assistance.

Appendix.—References

1. Albandar, F. A-A., and Mills, G. M., "The Prediction of Crack Widths in Reinforced Concrete Beams," *Magazine of Concrete Research*, Vol. 26, No. 88, Sept., 1974, pp. 153–160.
2. Base, G. D., Read, J. B., Beeby, A. W., and Taylor, H. P. J., "An Investigation of the Crack Control Characteristics of Various Types of Bar in Reinforced Concrete Beams," *Research Report No. 18*, Parts 1, 2, Cement and Concrete Association, London, England, Dec., 1966.
3. Bažant, Z. P., and Oh, B. H., "Concrete Fracture via Stress-Strain Relations," *Report No. 81-10/665*, Center for Concrete and Geomaterials, Northwestern University, Evanston, Ill., Oct., 1981.
4. Bažant, Z. P., and Oh, B. H., "Crack Spacing in Reinforced Concrete: Approximate Solution," *Journal of Structural Engineering*, ASCE, Vol. 109, No. 9, Sept., 1983, pp. 2207–2212.
5. Bažant, Z. P., and Oh, B. H., "Deformation of Cracked Net-Reinforced Concrete Walls," *Journal of Structural Engineering*, ASCE, Vol. 109, No. 1, Jan., 1983, pp. 93–108.
6. Bažant, Z. P., and Ohtsubo, H., "Stability Conditions for Propagation of a System of Cracks in a Brittle Solid," *Mechanics Research Communications*, Vol. 4, No. 5, Sept., 1977, pp. 353–366.
7. Bažant, Z. P., and Raftshol, W. J., "Effect of Cracking in Drying and Shrinkage Specimens," *Cement and Concrete Research*, 1982 (in press).
8. Bažant, Z. P., and Wahab, A. B., "Instability and Spacing of Cooling on Shrinkage Cracks," *Journal of the Engineering Mechanics Division*, ASCE, Vol. 105, No. EM5, Proc. Paper 14933, Oct., 1979, pp. 873–889.
9. Bažant, Z. P., and Wahab, A. B., "Stability of Parallel Cracks in Solids Reinforced by Bars," *International Journal of Solids and Structures*, Vol. 16, 1980, pp. 97–105.
10. Bažant, Z. P., Ohtsubo, H., and Aoh, K., "Stability and Post-Critical Growth of a System of Cooling or Shrinkage Cracks," *International Journal of Fracture*, Vol. 15, No. 5, Oct., 1979, pp. 443–456.
11. Broms, B. B., "Crack Width and Crack Spacing in Reinforced Concrete Members," *Journal of the American Concrete Institute*, Proceedings, Vol. 62, No. 10, Oct., 1965, pp. 1237–1256.
12. Broms, B. B., and Lutz, L. A., "Effects of Arrangement of Reinforcement on Crack Width and Spacing of Reinforced Concrete Members," *Journal of the American Concrete Institute*, Proceedings, Vol. 62, No. 11, Nov., 1965.

13. Chi, M., and Kirstein, A. F., "Flexural Cracks in Reinforced Concrete Beams," *Journal of the American Concrete Institute*, Proceedings, Vol. 54, No. 10, Apr., 1958, pp. 865–878.
14. Clark, A. P., "Cracking in Reinforced Concrete Flexural Member," *Journal of the American Concrete Institute*, Proceedings, Vol. 52, No. 8, Apr., 1956, pp. 851–862.
15. Fung, Y. C., *Foundations of Solid Merchanics*, Prentice Hall, Inc., Englewood Cliffs, N.J., 1965.
16. Gergely, P., and Lutz, L. A., "Maximum Crack Width in Reinforced Concrete Flexural Members," *Causes, Mechanism, and Control of Cracking in Concrete, SP-20*, American Concrete Institute, Detroit, Mich., 1968, pp. 87–117.
17. Hillerborg, A., Modéer, M., and Petersson, P. E., "Analysis of Crack Formation and Crack Growth in Concrete by Means of Fracture Mechanics and Finite Elements," *Cement and Concrete Research*, Vol. 6, 1976, pp. 773–782.
18. Hognestad, E., "High Strength Bars as Concrete Reinforcement, Part 2. Control of Flexural Cracking," *Journal of the Portland Cement Association Research and Development Laboratories*, Vol. 4, No. 1, Jan., 1962, pp. 46–63.
19. Kaar, P. H., and Hognestad, E., "High Strength Bars as Concrete Reinforcement, Part 7. Control of Cracking in T-Beam Flanges," *Journal of the Portland Cement Association Research and Development Laboratories*, Vol. 7, No. 1, Jan., 1965, pp. 42–53.
20. Kaar, P. H., and Mattock, A. H., "High Strength Bars as Concrete Reinforcement, Part 4, Control of Cracking," *Journal of the Portland Cement Association Research and Development Laboratories*, Vol. 5, No. 1, Jan., 1963, pp. 15–38.
21. Knott, J. F., *Fundamentals of Fracture Mechanics*, Butterworths, London, England, 1973.
22. Mathey, R. G., and Watstein, D., "Effect of Tensile Properties of Reinforcement on the Flexural Characteristics of Beams," *Journal of the American Concrete Institute*, Proceedings, Vol. 56, No. 12, June, 1960, pp. 1253–1273.
23. Meier, S. W., and Gergely, P., "Flexural Crack Width in Prestressed Concrete Beams," *Journal of the Structural Division*, ASCE, Vol. 107, No. ST2, Proc. Paper 16010, Feb., 1981, pp. 429–433.
24. Nawy, E. G., "Crack Control in Reinforced Concrete Structures," *Journal of the American Concrete Institute*, Proceedings, Vol. 65, No. 10, Oct., 1968, pp. 825–836.
25. Park, R., and Paulay, T., *Reinforced Concrete Structures*, John Wiley and Sons, New York, N.Y., 1975 (Section 10.4).
26. Petersson, P. E., "Fracture Energy of Concrete: Method of Determination," *Cement and Concrete Research*, Vol. 10, 1980, pp. 78–89, and "Fracture Energy of Concrete: Practical Performance and Experimental Results," *Cement and Concrete Research*, Vol. 10, 1980, pp. 91–101.
27. Sneddon, I. N., and Lowengrub, M., *Crack Problems in the Classical Theory of Elasticity*, John Wiley and Sons, New York, N.Y., 1969 (p. 134).
28. Tada, H., Paris, P. C., and Irwin, G. R., "The Stress Analysis of Cracks Handbook," Del Research Corp., Hellertown, Pa., 1973.
29. Watstein, D., and Mathey, R. G., "Width of Cracks in Concrete at the Surface of Reinforcing Steel Evaluated by Means of Tensile Bond Specimens," *Journal of the American Concrete Institute*, Proceedings, Vol. 56, No. 1, July, 1959, pp. 47–56.
30. Watstein, D., and Parsons, D. E., "Width and Spacing of Tensile Cracks in Axially Reinforced Concrete Cylinders," *Journal of Research of the National Bureau of Standards*, Vol. 31, July, 1943, No. RP545, pp. 1–24.